Journal of Intelligent System and Telecommunications

Journal homepage: https://journal.unesa.ac.id/index.php/jistel/index

Classification on Heart Rate Zone using SVM with Random Search: A Comparative Study with RF and XGBoost

Muhammad 'Aamir Nashrullah[1], *Pradini Puspitaningayu*[1*], *Hapsari Peni Agustin Tjahyaningtijas* [1], *Muhamad Bagus Fikril Alan*[1], *Yohanes Yohanie Fridelin Panduman*[2], *Lucy Widya Fathir*[3]

[1]Dept. of Electrical Engineering, Faculty of Engineering, Universitas Negeri Surabaya, Indonesia
[2] Graduate School of Information Science and Technology, Osaka University, Japan
[3]Faculty of Sports Science and Health, Universitas Negeri Surabaya, Indonesia

*Correspondence: E-mail: pradinip@unesa.ac.id

ARTICLE INFO

Article History:
Submitted/Received 11 June 2025
First Revised 22 June 2025
Accepted 30 June 2025
First Available Online 30 June 2025
Publication Date 30 June 2025

Keyword:
Machine Learning, Classification, SVM, RF, XGBoost, HR.

ABSTRACT

Classification of heart rate (HR) zones during resistance training plays a crucial role in precisely regulating exercise intensity to enhance the effectiveness and safety of fitness programs. This study proposes a machine learning-based framework with Support Vector Machine (SVM) as the primary model, optimized using the random search method. SVM was chosen due to its capability to separate high-dimensional data and capture subtle distinctions between HR zones, especially the transition between aerobic and anaerobic states. Experimental results demonstrate that SVM delivers the highest performance among all models tested, achieving an accuracy of 98%, supported by high precision, recall, and F1-score values, while exhibiting minimal misclassifications. Compared to Random Forest and XGBoost, which also show strong results, SVM maintains superior consistency and generalization across all zone categories. The main contribution of this research lies in applying an optimized SVM to time-series-based HR sensor data for multi-zone classification, enabling accurate real-time detection during workouts. Moreover, the proposed framework is designed for integration into wearable devices, paving the way for intelligent, personalized, and adaptive fitness monitoring. These findings establish a robust baseline for further exploration into ensemble learning and deep learning integration, with the goal of enhancing the performance and flexibility of heart rate zone detection systems.

1. INTRODUCTION

Weight training is acknowledged as a science-backed method for improving muscle strength, endurance, and overall fitness. Nonetheless, the elevated intensity and regularity of training sessions typically linked to these routines can hasten the emergence of fatigue, subsequently reducing movement efficiency, increasing the likelihood of injury, and impeding long-term performance enhancements [1]. Consequently, real-time and accurate monitoring of heart rate zones has become essential for designing safe and effective training programs.

Heart rate (HR) serves as a key physiological marker that provides direct insight into an individual's cardiovascular response during exercise [2]. By tracking HR zones, such as recovery, aerobic, anaerobic, and maximum effort coaches and sports practitioners can tailor training volume and intensity in real time to target specific energy systems [3]. This proactive approach helps optimize recovery, minimize the risk of overtraining, and underscore the importance of managing both physical and mental aspects of performance [4].

Heart rate zones are classified ranges that reflect different exercise intensities and their corresponding physiological effects. Accurate classification of these zones enables athletes to train within targeted intensities for endurance development, fat oxidation, or peak power output [5]. In practice, misclassification of HR zones may lead to suboptimal training adaptations or increased injury risk, which points to the importance of objective and reliable assessment methods [6]. Manual estimation of HR zones, based on formulas like the Karvonen method or percentage of maximum HR, can be prone to errors, paving the way for AI-based solutions to provide consistent and automated zone detection [7].

Advances in artificial intelligence (AI) and the growing availability of large-scale physiological data have transformed HR zone monitoring. Machine learning techniques excel at uncovering hidden patterns within raw biometric inputs such as time series HR data and converting them into actionable insights [8][9]. While ensemble learning algorithms have been widely adopted for their robustness against data complexity, properly optimized single models can also achieve high performance in classification tasks.

In this system for classifying heart rate zones, Support Vector Machine (SVM) is chosen as the main model due to its ability to handle high-dimensional time-series data and build optimal hyperplanes for multiclass classification [10][11]. Utilizing kernel functions like Gaussian RBF or polynomial, SVM enables the projection of data into higher-dimensional space, facilitating the separation of complex patterns in heart rate signals [12][13]. In addition to SVM, two comparative algorithms will be used: Random Forest (RF), which offers robustness against noisy data and provides feature importance estimation through the aggregation of multiple decision trees [14], and XGBoost, which utilizes regularized gradient boosting to enhance accuracy with high computational efficiency and the ability to handle imbalanced data [15]. The comparison of performance in terms of accuracy, precision, recall, and F1-score between SVM, RF, and XGBoost will reveal the extent to which a single optimized model compares with popular ensemble methods.

For hyperparameter optimization, this study adopts random search because it can explore a wide parameter space with random samples, thus increasing the chances of finding a near-optimal configuration compared to the structured but computationally expensive grid search [16][17]. By setting limits on the number of iterations and value ranges for each main hyperparameter, such as C and γ in SVM, the number of trees and maximum depth in RF, and the learning rate and number of boosting rounds in XGBoost, random search allows for more efficient exploration and reduces training time, without having to test every parameter combination exponentially [18].

The objective of this research is to develop a reliable HR zone classification system by leveraging SVM as the primary model and to benchmark its performance against RF and

DOI: https://doi.org/10.26740/jistel.v1n2.p162-174
e- ISSN 3090-613X

XGBoost. The resulting system is expected to be integrated into wearable devices or digital health applications, providing real-time HR zone detection and data-driven guidance for athletes and sports practitioners.

2. RELATED WORK

Many studies have already addressed classification problems using biological data. In this case, one of them is detecting fatigue using heart rate variability (HRV) data that can be applied in wearable devices for sports [19]. However, sometimes biological data is not only used in sports matters but also in general matters such as conducting research for fatigue detection in drivers using HRV and electrodermal activity data [20], which focuses on detecting driver fatigue using several models and 2 different datasets. So in this study, we aim to create a classifier using a lighter machine learning model with a heart rate dataset because, in previous research, the use of heart rate data for sports purposes was still very limited. With the heart rate dataset, it will facilitate future implementation since heart rate data can be obtained using sensors that are simple to use and widely available in the market, whereas using HRV data requires ECG or EEG sensors, which are relatively expensive.

3. METHODS

This research utilizes a machine learning framework to classify heart rate zones, recovery, normal, aerobic, anaerobic, and maximum effort during weight training sessions. As the main model, Support Vector Machine (SVM) was chosen due to its ability to separate high-dimensional data through an optimal hyperplane, while Random Forest (RF) and XGBoost were implemented as comparative models. These three algorithms were tested comparatively to provide complementary insights into the performance of HR zone classification, resulting in an accurate and reliable real-time detection system for athletes and sports practitioners.

3.1. Material

HR data is the main physiological parameter for monitoring cardiovascular response during weight training sessions. HR variability reflects changes in intensity levels and the dominant energy systems, ranging from the recovery zone to the maximum effort zone. In the context of resistance training, real-time monitoring of these zones is crucial to optimize training programs, prevent the risk of excessive fatigue, and maximize physiological adaptation [2].

In this study, HR data were collected using the Polar H10 sensor connected in real-time to the Squad Heart Rate application. This device was chosen for its high accuracy in measuring heart rate during intense physical activity. Each training session lasts between 30 to 60 minutes, with a sampling rate of 1 to 5 seconds per data point, resulting in a time-series rich in temporal information.

After preprocessing, each HR data point is labeled into five intensity zones according to the established heart rate ranges: recovery, normal, aerobic, anaerobic, and maximum effort. These labels become the target output in the classification task. SVM was chosen as the main model, thanks to its ability to separate high-dimensional data with an optimal hyperplane and its proven performance on multiclass classification problems. To conduct a comparative evaluation, two benchmark models, RF and XGBoost, were also implemented, allowing this study to assess the reliability of SVM in detecting heart rate zones during resistance training.

3.2 Method

3.2.1 Support Vector Machine (SVM)

In this study, the SVM serves as the meta-learner within a stacking ensemble, responsible for integrating the probabilistic outputs of RF and XGBoost [12]. Each input vector x_i is implicitly mapped into a higher-dimensional feature space via a kernel function $k(x,x') = \phi(x)^T\phi(x')$, enabling linear separation in the transformed domain without explicitly computing $\phi(x)$. The training objective is formulated as the following primal optimization problem:

$$\min_{w_i} \frac{1}{2}\|w\|^2 + C\sum_{i=1}^{n} \varepsilon_i \tag{1}$$

subject to

$$y_i(w\,\phi(x_i) + b) \geq 1 - \varepsilon_i, \varepsilon_i \geq 0, i = 1$$

where the term $\frac{1}{2}\|w\|^2$ enforces a maximally wide margin (since the geometric margin is inversely proportional to $\|w\|$), enhancing robustness to noise and overfitting. The slack variables ε_i permit controlled margin violations, each ε_i quantifies the degree by which sample I falls within the margin or is misclassified. The regularization parameter C balances the trade-off between margin width and training error, a larger C prioritizes minimizing misclassification at the expence of a narrower margin, whereas a smaller C favors a wider margin tolerating more slack. The constraint $y_i(w\,\phi(x_i) + b) \geq 1 - \varepsilon_i$ ensures that correctly classified points lie beyond the magin boundary or incure a penalty proportional to their violation [10].

Once the optimal w and b are obtained, the raw decision function $w\,\phi(x_i) + b$ provides signed distances to the hyperplane but does not directly correspond to class membership probabilities. To address this, platt scalling is applied:

$$P(\mathrm{y} = \mathrm{c}|\mathrm{x}) = \frac{1}{1+\exp(Af(x)+B)}, \tag{2}$$

Where parameters A and B are calibrated by minimizing the negative log-likelihood on a held-out validation set. This logistic transformation yields well-calibrated probabilities, facilitating the combination of SVM outputs with those of base learners in the stacking framework. In the context of heart rate zone classification, probability estimates allow for threshold adjustment and more nuanced decision-making under uncertainly [10].

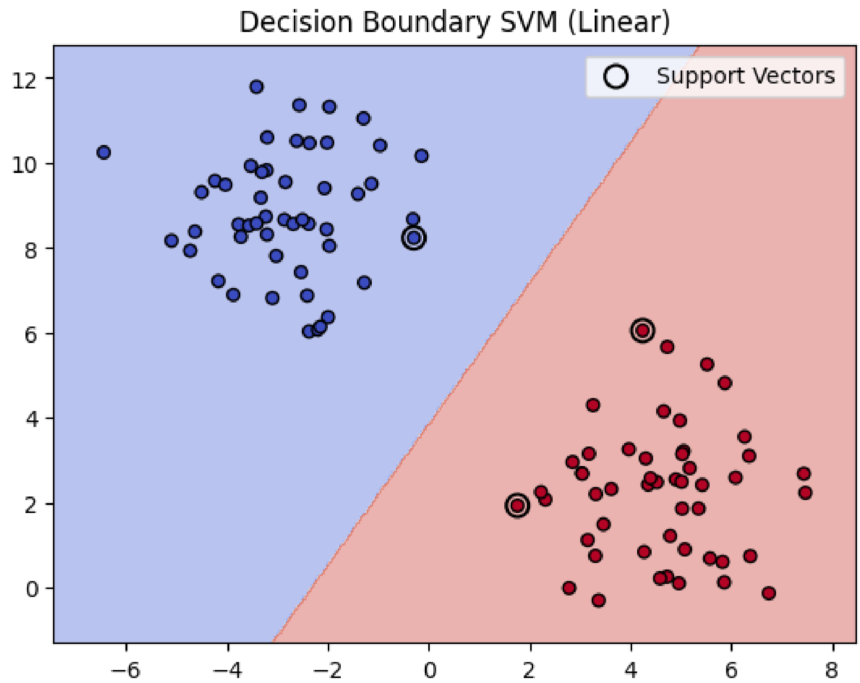

Figure 1. Decision Boundary of SVM model with linear kernel

DOI: https://doi.org/10.26740/jistel.v1n2.p162-174
e- ISSN 3090-613X

In **Figure 1**, the SVM hyperplane illustration depicts the decision boundary f(x) = 0 that separates two heart rate zone classes in the high dimensional kernel space. The circled point correspond to the support vectors, which are the training samples closest to the hyperplane and directly determine the orientation and position of the decision boundary [21]. By maximizing the separation margin among these support vectors, the SVM achieves strong generalization to unseen data, an essential property for accurately distinguishing subtle transitions between heart rate intensity zones during weight training sessions [11].

3.2.2 Random Forest (RF)

RF is employed in this study as one of the base learners within the stacking ensemble for heart rate zone classification during weight training. RF builds an ensemble of T decision trees by training each tree in a different bootstrap sample of the training data and selecting a random subset of features at each split, which ensures diversity among trees and reduces overfitting [14].

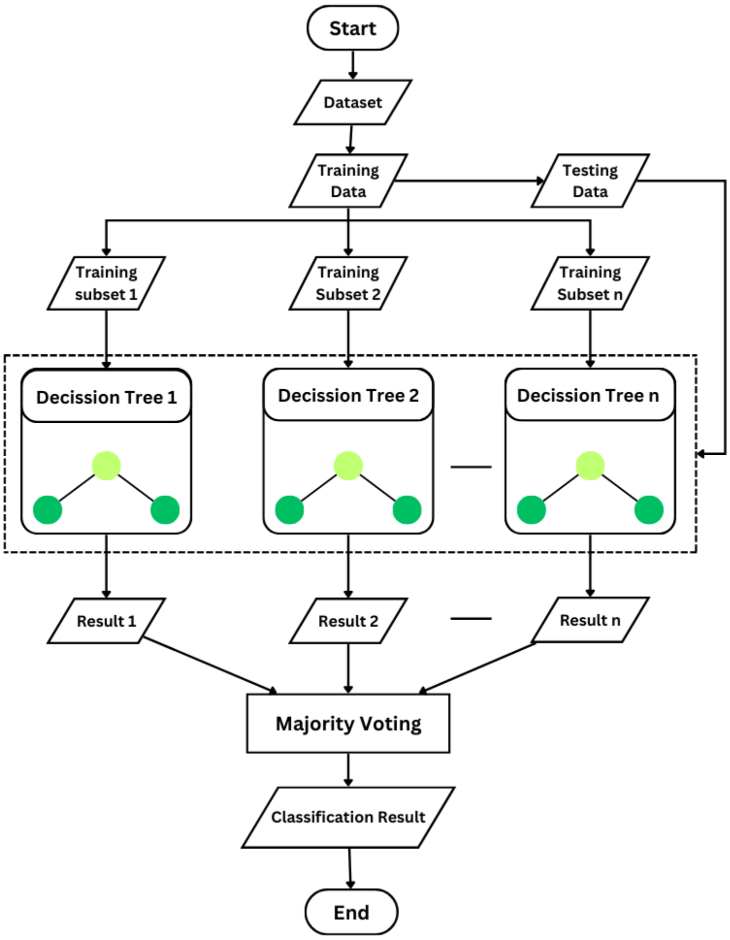

Figure 2. Random Forest Architecture

RF is a classical algorithm in ensemble learning, which trains multiple decision trees to build an ensemble classifier, as shown in **Figure 2**. Several different training subsets are obtained by sampling with replacement from the training set. Each training subset is used to train a decision tree, and multiple trained decision trees can form an ensemble classifier.

Each tree partitions its input space into a set of terminal nodes (leaves) L. The tree-level prediction for an input x is defined as:

$$f_t(x) = \frac{1}{|L|}\sum_{l\in L} I(x \in l), \tag{3}$$

Where $I(x \in l)$ is an indicator function that equals 1 if x falls into leaf l and 0 otherwise. In a classification setting $f_t(x)$ is interpreted as the proportion of training samples of the target class c in the leaf where x lands, effectively estimating $P_t(y = c|x)$ [22].

After all trees have produced their individual class, probability estimates, the overall RF prediction dor class c is obtained by averaging these per tree probabilities:

$$P_t(y = c|x) = \frac{1}{T}\sum_{t=1}^{T} P_t(y = c|x) \tag{4}$$

Where T is the total number of trees. The final class label is then chosen as the one with the highest average probability. This bagging procedure combining bootstrap sampling with model averaging significantly reduces variance compared to single decision tree and enhances robustness against noisy or outlier prone physiological data [23].

In **Figure 2,** each tree is trained on a bootstrapped subset of the data with random feature selection at each node, individual tree outputs are class probability estimates that are averaged to yield the final prediction [24].

In the context of heart rate zone classification, RF ability to capture complex, nonlinear relationships in the time series HR data makes it particularly effective at distinguishing between recovery, normal, aerobic, anaerobic, and maximum. By aggregating diverse decision boundaries across many trees, RF provides vomplementary insights alongside SVM and XGBoost, improving the overall stability and accuracy of the stacking ensemble.

3.2.3 XGBoost

The Extreme Gradient Boosting (XGBoost) is a new tree-based algorithm that has been increasing in popularity for data classification recently, that has been proved to be a highly effective method for data classification [15]. The core of XGBoost's learning process at iteration t is the minimization of the regularized objective [25]:

$$L^{(t)} = \sum_{i=1}^{n} l\left(y_i, \hat{y}_i^{(t-1)} + f_t(x_i)\right) + \pi(f_t), \tag{5}$$

Where l(.) denotes the chosen loss function typically the log loss for multiclass classification y_i is the true class label, $\hat{y}_i^{(t-1)}$ is the aggregated prediction up to the previous iteration, and f_t is the newly added regression tree. During the construction, XGBoost evaluates the gain of a candidate split to choose the optimal feature and threshold. For a node that would be split into left subset L and right subset R, gain is computed as [25]:

$$\mathrm{G} = \frac{\left(\sum_{i\epsilon L} g_i\right)^2}{\sum_{i\epsilon L} h_i+\lambda} + \frac{\left(\sum_{i\epsilon R} g_i\right)^2}{\sum_{i\epsilon R} h_i+\lambda} + \frac{\left(\sum_{i=1}^{n} g_i\right)^2}{\sum_{i=1}^{n} h_i+\lambda}, \tag{6}$$

Where g_i and h_i are the first and second derivatives (gradient and hessian) of the loss with respect to the current predicition. The regularization parameter λ stabilizes the denominator, ensuring that splits with low second order information are not overemphasized. A higher gain indicates a more effective split in reducing the overall objective.

Once all T trees are built, XGBoost produces raw scores $\hat{y}_{i,c}$ for each class c. these scores are transformed into class probabilities via the softmax function:

$$P_{XGB}(\mathrm{y} = \mathrm{c}|x_i) = \frac{\exp(\hat{y}_{i,c})}{\sum_{k=1}^{C}\exp(\hat{y}_{i,c})}, \tag{7}$$

DOI: https://doi.org/10.26740/jistel.v1n2.p162-174
e- ISSN 3090-613X

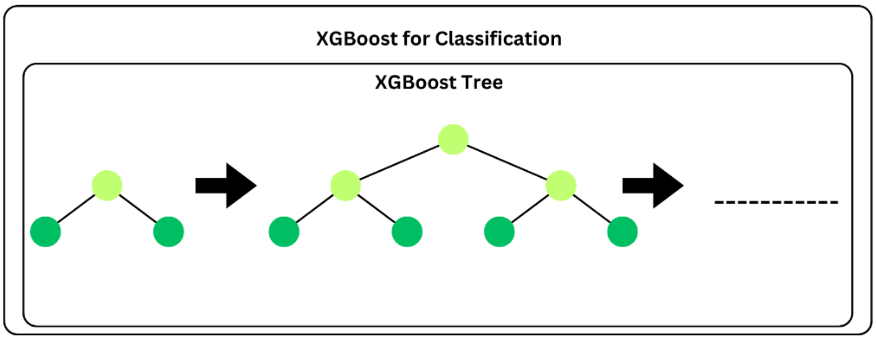

Figure 3. XGBoost architecture

In the eq (7) where C is the total number of heart rate zones. This probabilistic output allows direct integration with the stacking meta learner and support threshold based decision rules for delineating subtle transitions between recovery, normal, aerobic, anaerobic, and maximum [25].

In the **Figure 3**, at each iteration, a new tree f_t is grown to fit the negative gradients of the loss (residuals) from the previous iteration [26]. The model aggregates these trees sequentially, using the gain criterion (Eq. (6)) for optimal splits, and applies regularization (Eq. (5)) to control complexity. Final class probabilities are obtained via softmax (Eq. (7)).

3.2.4 Random Search

Random Search is a simple yet powerful black-box optimization technique in which a fixed budget of hyperparameter configurations is sampled uniformly at random from the search space. Unlike Grid Search whose number of trials grows exponentially with the number of hyperparameters Random Search's cost depends only on the predefined budget b, making it inherently scalable to high-dimensional problems and free from the curse of dimensionality . Because each trial is independent, Random Search can be trivially parallelized across multiple workers or devices without inter-process communication, which suits real-time or resource-constrained deployments [27].

Empirical studies across various deep-learning architectures demonstrate Random Search's practical effectiveness. In benchmark experiments on MNIST and CIFAR-10, Random Search consistently outperformed Manual Search and Grid Search in terms of accuracy and F1-score for MLP, CNN, and AlexNet models under a fixed computational budget. Notably, while Grid Search could fully explore small search spaces (e.g., MLP tuning within 7.35 hours), it became infeasible under tight time constraints for larger models, where Random Search's random sampling was more likely to locate high-performing configurations beyond the sequential grid order [28].

Despite its strengths, Random Search also exhibits limitations that warrant consideration. Its purely stochastic sampling can lead to inconsistent results across runs and may waste evaluations in regions of low performance, resulting in redundancy and inefficiency. Recent work advocates hybrid or adaptive variants such as slot-based sampling, genetic algorithms, or Bayesian-inspired heuristics to focus the search near promising areas while retaining broad coverage, thereby improving both convergence speed and reliability under constrained budgets.

3.3 Evaluation

In this research, a dataset of 940 data points is used, which will then be split into 80% training data and 20% testing data during the preprocessing stage. This division allows the model to achieve better performance because with a sufficient amount of training data, the machine learning model is very likely to produce the desired performance, which is an accuracy

DOI: https://doi.org/10.26740/jistel.v1n2.p162-174
e- ISSN 3090-613X

above 90%. Then, in the model training process in this research, Google Colab is used as the platform for programming and training, with the use of a virtual GPU and a stable internet connection to improve the training results.

To see the results of the model training, the model will be evaluated using several evaluation metrics, such as accuracy, precision, recall, and the F1 score. where these matrices are deemed suitable for use in classification problems by several published articles. So in this research, these evaluation matrices are used to determine whether the results of the model training meet the expectations through the calculations of each evaluation matrix.

3.3.1 Accuracy

Accuracy measures the overall correctness of the classifier by quantifying the ratio of all correctly predicted instances both true positives (TP) and true negatives (TN) to the total number of observations. It is calculated as [29]:

$$\text{Accuracy} = \frac{\text{TN+TP}}{\text{TN+TP+FN+FP}} \times 100\% \tag{8}$$

While accuracy offers an intuitive measure of performance, it can be misleading in imbalanced datasets where one class dominates, as high accuracy may hide poor detection of minority classes .

3.3.2 Precision

Precision indicates the percentage of correct positive predictions out of all instances predicted as positive by the model. It is computed by dividing the number of true positives (TP) by the total of true positives (TP) and false positives (FP) [29]:

$$Precision = \frac{TP}{\text{TP+FP}} \times 100\% \tag{9}$$

This metric is critical when the cost of false positives such as misguiding training intensity needs to be minimized.

3.3.3 Recall

Recall, or sensitivity, assesses the model's ability to correctly identify all actual positive instances. It captures the proportion of true positives relative to the sum of true positives and false negatives. High recall ensures that most true events of a target heart rate zone (e.g., anaerobic transitions) are detected. Recall is formulated as [29]:

$$Recall = \frac{TP}{\text{TP+FN}} \times 100\% \tag{10}$$

This metric is particularly important when missing a true positive (false negative) carries a significant risk, such as failing to detect a critical intensity zone.

3.3.4 F1-score

The F1 Score is a metric that provides a balanced assessment of precision and recall by calculating their harmonic mean. This metric is especially helpful when aiming to achieve a trade-off between high precision and high recall, as it penalizes cases where one metric is significantly lower than the other [29]:

$$f1 - score = 2 \times \frac{Precison \times Recall}{Precision + Recall} \times 100\% \tag{11}$$

By combining precision and recall, the F_1-Score is especially useful for comparing models when the distribution of errors between classes is uneven.

DOI: https://doi.org/10.26740/jistel.v1n2.p162-174
e- ISSN 3090-613X

4. RESULTS AND DISCUSSION

4.1. Results

Table 1 demonstrates that the SVM model achieved the highest overall accuracy (98 %), reflecting its ability to draw a clear decision boundary even in the presence of subtle overlaps between adjacent heart-rate zones. In **Figure 4**, the confusion matrix for SVM shows that nearly all samples fall along the diagonal, with only a handful of misclassifications occurring between the aerobic and anaerobic zones. This indicates that SVM's maximal-margin hyperplane effectively captures the nuanced feature differences that distinguish these two middle-intensity ranges. Moreover, the high precision (97 %) and recall (98 %) values confirm that, despite the potential challenge of class imbalance, SVM maintains both reliability of positive predictions and sensitivity to actual positive instances across all four zones.

The Random Forest model, with an accuracy of 95 %, exhibits greater stability during training due to its bagging procedure and feature subsetting. However, as seen in **Figure 5**, RF's confusion matrix reveals more off-diagonal entries compared to SVM. In particular, there is noticeable confusion between the recovery and aerobic zones, suggesting that some low-intensity heart-rate patterns share similar feature distributions that individual trees struggle to separate. RF's precision and recall metrics (95 % and 94 %, respectively) indicate that while it is generally reliable at predicting zones, it occasionally mislabels recovery samples as mild aerobic effort, which slightly diminishes its overall performance relative to SVM.

XGBoost attains 94% accuracy, closely following RF despite sharing a tree-based foundation. **Figure 6** shows that XGBoost excels at identifying maximum-effort zones likely due to its iterative correction of residuals but underpredicts the anaerobic zone more often than RF. This is reflected in its lower precision (93 %) and F_1-score (93 %), where false negatives in the anaerobic class reduce the model's sensitivity to that critical middle-high intensity range. The comparison between RF and XGBoosjt suggests that while boosting can capture complex, non-linear interactions within the heart-rate time series, it may introduce bias toward the majority or easiest-to-predict zones without careful regularization and hyperparameter tuning. Overall, these observations underscore the complementary strengths of the three approaches and highlight why SVM's robust boundary definition yields superior performance in heart-rate zone classification.

Table 1. Results of each model

Model	Accuracy	Precision	Recall	F1-score
SVM	98%	97%	98%	98%
RF	95%	95%	94%	95%
XGBoost	94%	93%	94%	93%

DOI: https://doi.org/10.26740/jistel.v1n2.p162-174
e- ISSN 3090-613X

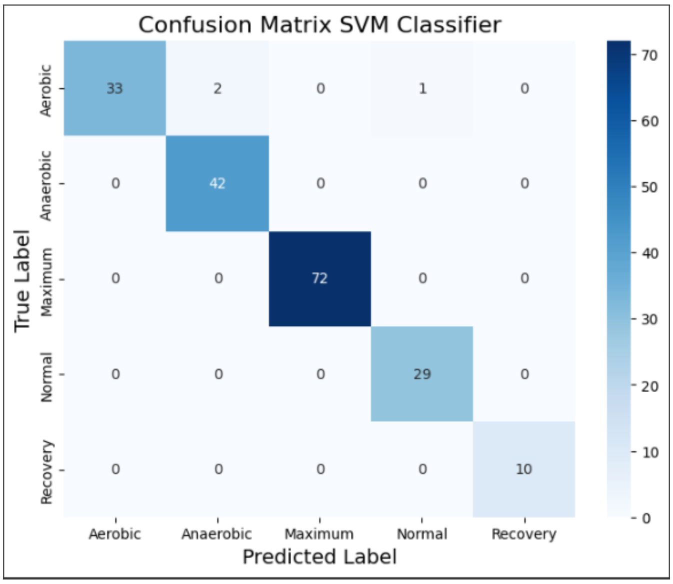

Figure 4. Confusion matrix SVM model

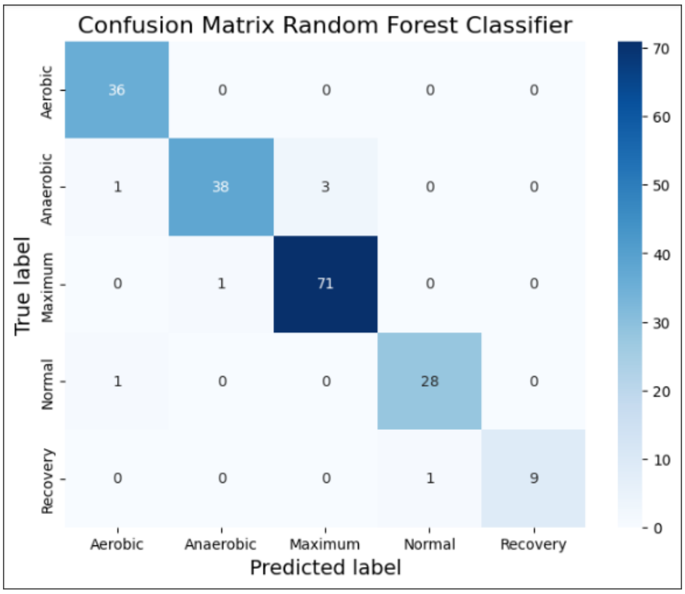

Figure 5. Confusion matrix RF model

DOI: https://doi.org/10.26740/jistel.v1n2.p162-174
e- ISSN 3090-613X

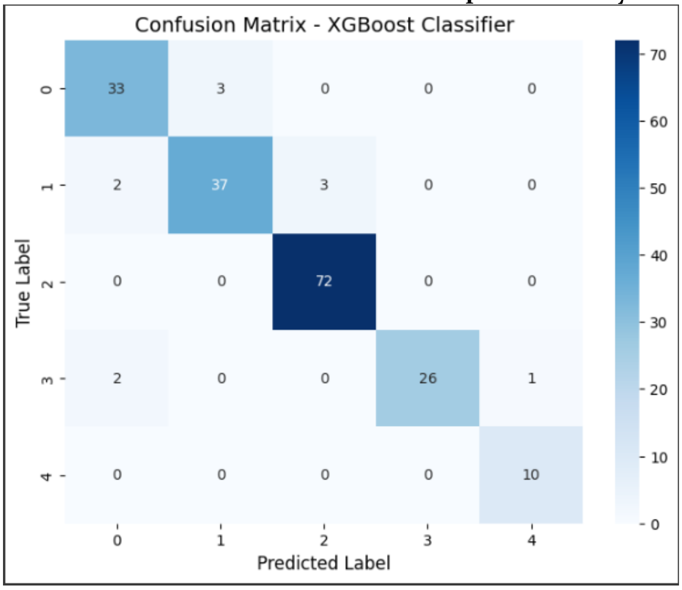

Figure 6. Confusion matrix XGBoost

5. CONCLUSION

The comparative evaluation of SVM, Random Forest, and XGBoost for heart-rate zone classification during weight-training revealed that SVM consistently outperforms the other models, achieving 98 % accuracy alongside the highest precision, recall, and F_1-score. Its maximal-margin hyperplane effectively separates the subtleties between adjacent intensity zones particularly aerobic and anaerobic resulting in minimal misclassifications as evidenced by the sparse off-diagonal entries in the SVM confusion matrix.

Random Forest demonstrated strong stability and robust handling of noisy, high-dimensional heart-rate features, securing 95 % accuracy. However, its tendency to confuse lower-intensity recovery and mild aerobic samples suggests that individual tree boundaries may overlap for similar physiological patterns. XGBoost, at 94 % accuracy, excelled in detecting extreme-intensity (maximum) zones but underperformed in the anaerobic class, indicating that its residual-correction mechanism may bias toward more distinct or majority classes without further hyperparameter refinement.

Thus, although all three approaches demonstrate high performance, the clear decision boundary of SVM makes it the most reliable for real-time heart rate zone detection. Future work will focus on integrating these models into an ensemble stacking that leverages their complementary strengths and exploring adaptive hyperparameter strategies to further enhance classification robustness across various athlete populations and training conditions. Additionally, these models will be combined with deep learning models to see how their performance compares to the baseline models. Furthermore, there will be an implementation in a health monitoring application during exercise to be utilized by trainers and athletes in monitoring heart rate zones.

6. ACKNOWLEDGMENT

This research was supported by the Institute for Research and Community Service (LPPM), the Sports and Exercise Research Center (SERC), and the Faculty of Engineering Universitas Negeri Surabaya (UNESA). The authors gratefully acknowledge the funding and resources provided, which made this study possible.

7. AUTHORS' NOTE

The authors declare that there is no conflict of interest regarding the publication of this article. The authors confirmed that the paper was free of plagiarism.

8. AUTHORS' CONTRIBUTION/ROLE

Muhammad Aamir Nashrullah: Conceptualization, Methodology, Writing Original Draft; Pradini Puspitaningayu: Formal Analysis, Data Curation, Writing Original Draft, Supervision; Hapsari Peni Agustin Tjahyaningtijas: Formal analysis, Review and Editing; Muhamad Bagus FIkril Alan: Formal Analysis, Writing Original Draft; Yohanes Yohanie Fridelin Panduman: Formal Analysis Review and Editing, Investigation; Lucy Widya Fathir: Data Curation, Investigation.

9. REFERENCES

[1] Yendrizal, Y. Kiram, R. Yenes, A. Komaini, N. Ihsan, and D. T. Mario, "Effect of weight training and motor skills on muscle strength: A factorial experimental design," *J. Phys. Educ. Sport*, vol. 23, no. 6, 2023, doi: 10.7752/jpes.2023.06173.

[2] C. Hernandez Engelhart *et al.*, "Reliability and agreement in intrapartum fetal heart rate monitoring interpretation: A systematic review," 2023. doi: 10.1111/aogs.14591.

[3] B. Dhananjay and J. Sivaraman, "Analysis and classification of heart rate using CatBoost feature ranking model," *Biomed. Signal Process. Control*, vol. 68, 2021, doi: 10.1016/j.bspc.2021.102610.

[4] D. Yu, M. Bouazizi, and T. Ohtsukil, "Improving Heart Rate Range Classification Using Doppler Radar with GAN-based Data Augmentation," in *Proceedings - IEEE Global Communications Conference, GLOBECOM*, 2023. doi: 10.1109/GLOBECOM54140.2023.10436801.

[5] A. Aguirre, M. J. Pinto, C. A. Cifuentes, O. Perdomo, C. A. R. Díaz, and M. Múnera, "Machine learning approach for fatigue estimation in sit-to-stand exercise," *Sensors*, vol. 21, no. 15, 2021, doi: 10.3390/s21155006.

[6] M. T. O. Worsey, H. G. Espinosa, J. B. Shepherd, and D. V. Thiel, "One Size Doesn't Fit All: Supervised Machine Learning Classification in Athlete-Monitoring," *IEEE Sensors Lett.*, vol. 5, no. 3, 2021, doi: 10.1109/LSENS.2021.3060376.

[7] L. Marotta, J. H. Buurke, B. J. F. van Beijnum, and J. Reenalda, "Towards machine learning-based detection of running-induced fatigue in real-world scenarios: Evaluation of IMU sensor configurations to reduce intrusiveness," *Sensors*, vol. 21, no. 10, 2021, doi: 10.3390/s21103451.

[8] M. Usman *et al.*, "Heart rate detection and classification from speech spectral features using machine learning," *Arch. Acoust.*, vol. 46, no. 1, 2021, doi: 10.24425/aoa.2021.136559.

[9] M. G. Signorini, N. Pini, A. Malovini, R. Bellazzi, and G. Magenes, "Integrating machine learning techniques and physiology based heart rate features for antepartum fetal monitoring," *Comput. Methods Programs Biomed.*, vol. 185, 2020, doi: 10.1016/j.cmpb.2019.105015.

[10] S. Dong, "Multi class SVM algorithm with active learning for network traffic classification," *Expert Syst. Appl.*, vol. 176, 2021, doi: 10.1016/j.eswa.2021.114885.

[11] R. I. Trisanti, A. Nizar, and D. Nur, "Journal of Intelligent System and Predicting Regional Sanitation Conditions Using Support Vector Machines and Neural Networks," vol. 1, pp. 41–50, 2024.

[12] X. Wu, Y. Zhou, and H. Xing, "Studies on the evaluation of college classroom teaching quality based on SVM multiclass classification algorithm," in *Journal of*

Physics: Conference Series, 2021. doi: 10.1088/1742-6596/1735/1/012011.
[13] D. Keerthana, V. Venugopal, M. K. Nath, and M. Mishra, "Hybrid convolutional neural networks with SVM classifier for classification of skin cancer," *Biomed. Eng. Adv.*, vol. 5, 2023, doi: 10.1016/j.bea.2022.100069.
[14] L. Sathish kumar, V. Pandimurugan, D. Usha, M. Nageswara Guptha, and M. S. Hema, "Random forest tree classification algorithm for predicating loan," *Mater. Today Proc.*, vol. 57, 2022, doi: 10.1016/j.matpr.2021.12.322.
[15] X. Deng, M. Li, S. Deng, and L. Wang, "Hybrid gene selection approach using XGBoost and multi-objective genetic algorithm for cancer classification," *Med. Biol. Eng. Comput.*, vol. 60, no. 3, 2022, doi: 10.1007/s11517-021-02476-x.
[16] D. A. Anggoro and S. S. Mukti, "Performance Comparison of Grid Search and Random Search Methods for Hyperparameter Tuning in Extreme Gradient Boosting Algorithm to Predict Chronic Kidney Failure," *Int. J. Intell. Eng. Syst.*, vol. 14, no. 6, 2021, doi: 10.22266/ijies2021.1231.19.
[17] L. Villalobos-Arias and C. Quesada-López, "Comparative study of random search hyper-parameter tuning for software effort estimation," in *PROMISE 2021 - Proceedings of the 17th International Conference on Predictive Models and Data Analytics in Software Engineering, co-located with ESEC/FSE 2021*, 2021. doi: 10.1145/3475960.3475986.
[18] M. Dhilsath Fathima and S. J. Samuel, "Hyperparameter tuning of ensemble classifiers using grid search and random search for prediction of heart disease," in *Computational Intelligence and Healthcare Informatics*, 2021. doi: 10.1002/9781119818717.ch8.
[19] C. Goumopoulos and N. Potha, "Mental fatigue detection using a wearable commodity device and machine learning," *J. Ambient Intell. Humaniz. Comput.*, vol. 14, no. 8, 2023, doi: 10.1007/s12652-021-03674-z.
[20] Y. Jiao, C. Zhang, X. Chen, L. Fu, C. Jiang, and C. Wen, "Driver Fatigue Detection Using Measures of Heart Rate Variability and Electrodermal Activity," *IEEE Trans. Intell. Transp. Syst.*, vol. 25, no. 6, 2024, doi: 10.1109/TITS.2023.3333252.
[21] R. Hooda, V. Joshi, and M. Shah, "A comprehensive review of approaches to detect fatigue using machine learning techniques," 2022. doi: 10.1016/j.cdtm.2021.07.002.
[22] L. Gaur *et al.*, "Disposition of Youth in Predicting Sustainable Development Goals Using the Neuro-fuzzy and Random Forest Algorithms," *Human-centric Comput. Inf. Sci.*, vol. 11, 2021, doi: 10.22967/HCIS.2021.11.024.
[23] A. Naseer and A. Jalal, "Pixels to Precision: Features Fusion and Random Forests over Labelled-based Segmentation," *Proc. 2023 20th Int. Bhurban Conf. Appl. Sci. Technol. IBCAST 2023*, no. October, pp. 1–6, 2023, doi: 10.1109/IBCAST59916.2023.10712869.
[24] L. Wan, K. Gong, G. Zhang, X. Yuan, C. Li, and X. Deng, "An efficient rolling bearing fault diagnosis method based on spark and improved random forest algorithm," *IEEE Access*, vol. 9, 2021, doi: 10.1109/ACCESS.2021.3063929.
[25] A. V. Konstantinov and L. V. Utkin, "A Generalized Stacking for Implementing Ensembles of Gradient Boosting Machines," in *Studies in Systems, Decision and Control*, vol. 350, 2021. doi: 10.1007/978-3-030-67892-0_1.
[26] X. Y. Liew, N. Hameed, and J. Clos, "An investigation of XGBoost-based algorithm for breast cancer classification," *Mach. Learn. with Appl.*, vol. 6, 2021, doi: 10.1016/j.mlwa.2021.100154.
[27] A. Esmaeili, Z. Ghorrati, and E. T. Matson, "systems Tuning and Global Function Optimization †," 2023.
[28] A. R. M. Rom, N. Jamil, and S. Ibrahim, "Multi objective hyperparameter tuning via random search on deep learning models," *Telkomnika (Telecommunication Comput. Electron. Control.*, vol. 22, no. 4, pp. 956–968, 2024, doi:

10.12928/TELKOMNIKA.v22i4.25847.

[29] A. A. Mon and U. N. Surabaya, “Journal of Intelligent System and SURFACE DETECTION FOR QUADRUPED ROBOT USING YOLO-V3 TINY,” vol. 1, pp. 13–24, 2024.

DOI: https://doi.org/10.26740/jistel.v1n2.p162-174
e- ISSN 3090-613X